

ORIGINAL ARTICLE

Promotion of reversible Li⁺ storage in transition metal dichalcogenides by Ag nanoclusters

Ge Ji¹, Yong Yu¹, Qiaofeng Yao¹, Baihua Qu¹, Dongyun Chen¹, Weixiang Chen², Jianping Xie¹ and Jim Yang Lee¹

After years of development, improvement in the electrochemical properties of MoS₂ through structural modifications has reached its limit. Further improvements in the Li⁺ storage properties of MoS₂ must be based on an understanding of the Li⁺ storage mechanism in MoS₂. On this basis, we have developed a novel ternary composite of graphene, MoS₂ nanosheets and a small amount (1 wt%) of silver nanoclusters (NCs; MoS₂/G/Ag). The presence of the Ag NCs in the composite is, however, instrumental and serves several purposes: immobilization of sulfur, increased association with Li⁺ and increased spacing between graphene sheets. The presence of this small amount of Ag NCs was able to increase the Li⁺ storage capacity of MoS₂ by 60% (with a discharge capacity of ~1300 mAh g⁻¹ at 0.5 A g⁻¹ compared with 800–850 mAh g⁻¹ for a MoS₂/graphene composite without the Ag NCs (MoS₂/G)). The MoS₂/G/Ag composite also exhibited a very impressive rate performance: discharge capacities of 1040 and 850 mAh g⁻¹ at the very high current densities of 1 and 5 A g⁻¹, respectively (the corresponding values from MoS₂/G without the Ag NCs are 790 and 580 mAh g⁻¹).

NPG Asia Materials (2016) 8, e247; doi:10.1038/am.2016.21; published online 18 March 2016

INTRODUCTION

It has been established in the lithium-ion battery (LIB) community that layered two-dimensional nanomaterials are efficient structures for the reversible storage of Li⁺. The common graphite anode is a good example. Graphite, however, comes with the disadvantage of its capacity being limited by the LiC₆ stoichiometry (372 mAh g⁻¹). There is, therefore, a strong motivation to search for high-capacity alternatives to graphite. MoS₂, a layered transition-metal dichalcogenide, has drawn the most interest. MoS₂ consists of a layer of hexagonally packed Mo atoms between two S layers, which is repeated *ad infinitum*. The Mo–S interaction is covalent in character and strong, whereas the interaction between adjacent S layers is governed by weak van der Waals forces.^{1–7} MoS₂ has to be suitably exfoliated to be an effective Li⁺ storage host. Exfoliated MoS₂ has shown a capacity of ~950 mAh g⁻¹ at 50 mA g⁻¹ for at least 100 cycles.^{8,9}

The electrochemical performance of MoS₂ can be further improved by the formation of a composite with graphene.^{10–14} Graphene (G), an intrinsic two-dimensional material, is often introduced during the MoS₂ synthesis to guide the formation of MoS₂ sheets and create a sheet-on-sheet or sheets-on-sheets heterostructure. The compatible geometry between transition-metal dichalcogenide and graphene leads to a stable composite with good conductivity and very little capacity fading during charge and discharge operations.^{15,16} Previous studies have suggested that the electrochemical performance of MoS₂/graphene composites as a LIB anode material is strongly dependent

on the structure, especially the layer thickness.^{10,11} MoS₂/graphene composites with different layer thicknesses could be formed by hydrothermal synthesis or reflux methods.^{17–20} The composites with better performance can deliver a capacity of 1000–1200 mAh g⁻¹ at 0.1 A g⁻¹ and ~700–800 mAh g⁻¹ at 1 A g⁻¹. After years of development, the improvement of the electrochemical performance of MoS₂ through structural modifications has probably reached its limits. Further improvements of the Li⁺ storage properties of MoS₂ would have to be based on an understanding of the Li⁺ storage mechanism in MoS₂. The reactions involved in the storage process are still not well understood, although more is known today than was known previously. There is increasing evidence for MoS₂ decomposition when it is discharged (lithiated) below 1.1 V vs Li/Li⁺ (MoS₂+4Li⁺→Mo+2Li₂S).^{10,14,21} The reaction is irreversible and yields Li₂S and Mo. Subsequent charging and discharging, therefore, cycles the battery like a Li-S cell (S+2Li⁺↔Li₂S). Amazingly, the ‘Li-S cell’ formed as such is free from some of the greatest challenges in the Li-S system: the low conductivity of S and the notorious polysulfide shuttle effect during discharge and charge. Although a MoS₂-derived Li-S cathode does not have the high gravimetric capacity of S (1672 mAh g⁻¹), its capacity fading is significantly lower than that of a typical Li-S cell. It is believed that the Mo from MoS₂ decomposition contribute to the increase in conductivity of an otherwise insulating Li₂S matrix. Disperse Mo atoms may also act as pinning sites for the polysulfides to suppress

¹Department of Chemical and Biomolecular Engineering, National University of Singapore, Singapore and ²Department of Chemistry, Zhejiang University, Hangzhou, China
Correspondence: Professor JY Lee, Department of Chemical and Biomolecular Engineering, National University of Singapore, 10 Kent Ridge Crescent, Singapore 119260, Singapore.

E-mail: cheleejy@nus.edu.sg

Received 30 June 2015; revised 17 December 2015; accepted 6 January 2016

their migration from the cathode.^{10,21} The capacity of MoS₂ based on the S+2Li⁺⇌Li₂S reaction is, theoretically, 669 mAh g⁻¹. The experimentally measured specific capacities are often larger than this value, with the extra capacity often attributed to the association of Li⁺ with Mo.^{10,21} A recent review article noted that nanostructured molybdenum particles may also participate in the lithiation reaction to some extent, serving as physical adsorption sites for the Li ions.²¹ Such a property may not be unique to Mo, and it is likely that other metal nanoparticles, or even nanoclusters (NCs), may also associate with Li⁺.

We report here a further modification of the MoS₂/graphene Li⁺ storage system based on the current understanding of the storage mechanism and the additional presence of a small amount (1 wt%) of Ag NCs. The new ternary composite prepared in this way, denoted as MoS₂/G/Ag, showed by far the best performance among the MoS₂ family of LIB anodes (stable discharge capacity of ~1300 mAh g⁻¹ at 0.5 A g⁻¹ and ~850 mAh g⁻¹ at 5 A g⁻¹). The Ag NCs used in our design are small (<2 nm) Ag nanoparticles that have been reported to display molecular-like properties and some promising features for a wide range of applications.^{22–27} Ag NCs were chosen for a number of reasons, including (1) the strong binding between Ag and S, (2) the large surface area of NCs compared with nanoparticles, which could reduce the usage of Ag, and (3) the fact that the small size of Ag NCs may allow them to be inserted into the gallery space between the MoS₂ layer and the graphene layer. The measured high-capacity and high-rate performance of the MoS₂/G/Ag composite aptly demonstrated the effectiveness of the NC modification in enhancing the performance of transition-metal dichalcogenide-based LIB anode materials. The Ag NC enhancement effects, including the immobilization of S, the association of Li⁺, and the increase in the distance between the graphene sheets (Figure 1), are presented in detail in the following section.

MATERIALS AND METHODS

Materials synthesis and characterization

Preparation of graphene oxide (GO). GO was prepared from the oxidation of natural graphite flakes using the modified Hummers' method.²⁸ In a typical preparation, a mixture of graphite powder (0.1 g), potassium permanganate (6 g) and concentrated sulfuric acid (40 ml) was placed in an ice-water bath and stirred for 2 h. The mixture was then diluted with 50 ml of deionized water, followed by the slow addition of 10 ml of H₂O₂ (30 wt% aqueous solution). The suspension was filtered 10 min later, and the solid residue was washed with deionized water four times. The washed solid was redispersed in 40 ml of deionized water and subjected to intense ultrasonication for 30 min.

Preparation of Ag NC decorated GO (GO/Ag). The preparation of Ag NCs was based on the CO-reduction method.²⁹ In a typical synthesis, an aqueous AgNO₃ solution (4 ml, 0.01 M) was added to a stirred GO suspension (80 ml, 0.625 mg ml⁻¹). Stirring continued for a further 30 min before CO gas at 1 bar pressure was bubbled through the mixture at room temperature under vigorous stirring for 5 min to saturate the mixture with CO. Later, the mixture was sealed, and a GO/Ag composite could be formed after resting for 3 h.

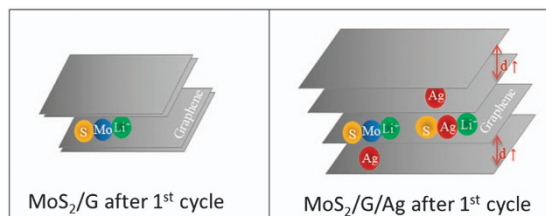


Figure 1 A schematic of MoS₂/G and MoS₂/G/Ag composite structures after the first cycle.

Preparation of MoS₂/G/Ag composite. A solution of 0.52 g (2 mmol) (NH₄)₂MoS₄ in 40 ml deionized water was introduced to the GO/Ag composite solution prepared by the method described above. 10 ml of hydrazine hydrate (85%) was then added as a reducing agent under constant stirring. The reaction mixture was refluxed at 95 °C for 12 h. The solid product recovered from the suspension by centrifugation was washed with deionized water and freeze dried. Finally, the dry solid was heat-treated in flowing nitrogen at 800 °C for 2 h to yield the Ag NC-MoS₂-G ternary composite (denoted as MoS₂/G/Ag). For comparison, the Ag-free MoS₂/graphene nanosheet composite was also prepared by replacing GO/Ag with GO in the synthesis (denoted as MoS₂/G).

The morphology of samples was examined by high-resolution transmission electron microscopy (TEM) on a JEOL JEM-2100F microscope (JEOL, Tokyo, Japan) operating at 200 kV and by field emission scanning electron microscopy on a JEOL JSM-6700 F microscope (JEOL) operating at 5 kV. The identification of phases in the composites was based on powder X-ray diffraction, which was conducted on a Shimadzu XRD-6000 diffractometer (Shimadzu, Kyoto, Japan) using a Cu-K_α source. Ultraviolet–visible spectra were recorded by a Shimadzu UV-1800 spectrometer (Shimadzu).

Electrochemical tests. Two-electrode coin cells (type 2032) were assembled in an argon-filled glove box using the MoS₂ composite as the positive electrode, Li metal as the negative electrode, a Celgard 2400 separator and an electrolyte of 1 M LiPF₆ in EC+DEC (1:1 (w/w)) with a 5 wt% of fluoroethylene carbonate additive. The positive electrode was fabricated by slurry coating using a mixture of 80 wt% active material, 10 wt% acetylene black and 10 wt% polyvinylidene fluorides in *N*-methyl-2-pyrrolidinone. The mass loading of the electrode was ~1.3 mg cm⁻². The cycle stability of the cells was tested on a battery tester (NEWARE BTS-5 V, Neware Technology Co., Ltd., Shenzhen, China) at different current densities in the 0.01–3 V voltage window. Cyclic voltammetry at 0.1 mV s⁻¹ was used to identify the redox reactions in the 0–3 V (versus Li/Li⁺) voltage window on an AutoLab Electrochemical System. The AutoLab was equipped with a FRA2 type III attachment, and electrochemical impedance spectroscopy was carried out in the 100 kHz–0.1 Hz frequency range using a perturbation of 5 mV AC about the selected potentials. For the electrochemical impedance spectroscopy measurements of the cycled cells, a cell was cycled to the predetermined number of cycles at 0.5 A g⁻¹, and then electrochemical impedance spectroscopy measurements were carried out.

RESULTS AND DISCUSSION

The fabrication of the MoS₂/G/Ag composite involved a number of sequential steps (Supplementary Figure S1): the preparation of GO using a modified Hummer's method, the decoration of the GO sheets with Ag NCs formed using the carbon monoxide (CO)-reduction method; the deposition of MoS₂ nanosheets on GO sheets using the interaction between the oxygen-containing functional groups of GO and the Mo precursor to generate a sheet-on-sheet structure, and a finishing heat treatment in N₂ at 800 °C for 2 h to increase the MoS₂ crystallinity. The preparation of GO sheets and the deposition of MoS₂ sheets on them were based on previously published procedures.^{11,30} The uniform deposition of Ag NCs on the GO sheets is the key design feature of this study. It is important to distinguish the product of this step, the GO/Ag composite, from the common Ag nanoparticle/graphene composites that are formed by reacting AgNO₃ and GO with poly(*N*-vinyl-2-pyrrolidone) or tannic acid reducing-cum-stabilizing agent.^{31,32} The Ag nanoparticles in the latter are too large to be stabilized in the sheet-on-sheet layered structure formed by graphene and MoS₂ nanosheets. Nano-Ag much smaller in size than the Ag nanoparticles, that is, Ag NCs, can be formed by using gaseous CO to reduce Ag⁺ ions. CO has been shown in previous studies to provide a mild and controllable reaction environment suitable for the growth of Ag(0) in the cluster size range.^{29,33} The NCs in our preparation were stabilized using the GO functional groups (-COOH, -OH) as capping agents to restrain the growth of Ag NCs and to provide fine control of the cluster size. Hence, by simply bubbling CO through a GO

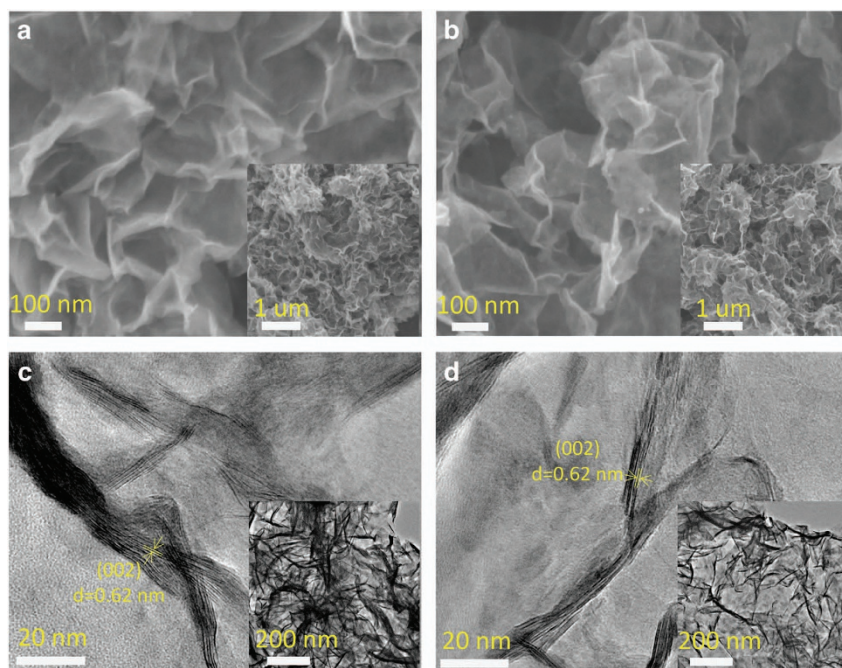


Figure 2 (a, b) Scanning electron microscopy, (c, d) high-resolution transmission electron microscopy images of MoS₂/G (a, c) and MoS₂/G/Ag (b, d). The insets correspond to lower magnification images of the same areas.

suspension containing AgNO₃, a GO/Ag composite could be formed quite readily. A representative TEM image of the GO/Ag composite (Supplementary Figure S2a) confirms the presence of Ag NCs as small (<2 nm), highly monodisperse particles on the GO sheets. The existence of Ag NCs is also supported by ultraviolet–visible spectroscopy (Supplementary Figure S2b), which showed only absorption peaks attributable to GO without the characteristic surface plasmon resonance peak of Ag nanoparticles at ~420 nm.

Figure 2 shows the general morphology of MoS₂/G (Figures 2a,b) and MoS₂/G/Ag (Figures 2c,d) by sampling over relatively large areas. Both composites exhibited a 3D architecture that could be attributed to graphene self-assembly during reflux. This is because the flexibility of the GO sheets allowed partial overlap or coalesce into the third dimension with relative ease before the reduction to graphene by hydrazine.¹¹ It can be seen from the TEM images that both composites contained thin micrometre-long sheets. The TEM images also show MoS₂ layers with an interlayer distance of 0.62 nm. A closer examination of the morphologies of MoS₂/G/Ag and MoS₂/G revealed systematically smaller numbers of layers in the MoS₂ sheets in the former (5–10 layers) compared with the latter (5–20 layers). This is an indication that Ag NCs had interfered with the stacking of MoS₂ layers during the synthesis of MoS₂/G/Ag composite. The small Ag NCs in the MoS₂/G/Ag composite were difficult to observe directly in the TEM images because they were located mostly between the graphene and MoS₂ layers and, as a result, were difficult to detect, even by high-resolution TEM (Figures 2c,d). Their presence could, however, be confirmed positively by XPS analysis in the Ag 3d binding energy region (Supplementary Figure S3). The presence of Ag NCs in MoS₂/G/Ag could also be confirmed by energy-dispersive X-ray spectroscopy (EDX) elemental mapping under the annular dark-field scanning transmission electron microscopy mode. Figure 3 shows a typical annular dark-field scanning transmission electron microscopy image of a MoS₂/G/Ag particle and the corresponding elemental maps of C, Ag, Mo and S. The uniform distribution of Ag throughout the

composite was confirmed by comparing the elemental maps. The elemental composition of MoS₂/G/Ag is summarized in the Table in the Figure. The calculated atomic ratio of S to Mo of 2.2 is close to the molecular formula of MoS₂. There was only 1 wt% of Ag in the composite. Although the quantification of EDX elemental mapping may be subject to some measurement errors, the calculated value of 1 wt% nonetheless indicates that the presence of Ag NCs in the composite is small. The EDX elemental maps of (Ag-free) MoS₂/G are shown in Supplementary Figure S4. Other than the obvious omission of Ag, its composition in terms of Mo, S and C was similar to that of MoS₂/G/Ag. The powder X-ray diffraction patterns of MoS₂/G and MoS₂/G/Ag are shown in Supplementary Figure S5. All of the diffraction peaks in the two composites could be indexed to hexagonal MoS₂ (JCPDS 37–1492). According to previous research, the absence of the MoS₂ (002) diffraction in MoS₂/G and MoS₂/G/Ag is an indication of the limited stacking of MoS₂ layers in the *c*-direction upon integration with graphene.^{9,13,34} The literature also assigns the peak at ~16° to the insertion of single-atom carbon between the MoS₂ sheets.³⁴ Similarly, the (002) diffraction peak of graphene was not detectable because of the comingling of graphene and MoS₂ layers in these composites. No Ag diffraction peak was found in MoS₂/G/Ag because the amount of Ag NCs in this composite was too small to produce to a coherent diffraction signal. Nonetheless, EDX elemental mapping has confirmed the presence of Ag in this composite; hence, it is reasonable to infer the existence of Ag NCs in MoS₂/G/Ag.

The cyclability of MoS₂/G and MoS₂/G/Ag in the discharge (lithiation) and charge (delithiation) processes was evaluated at constant current density (50 mA g⁻¹ for the first cycle and 500 mA g⁻¹ thereafter; Figure 4a). The first cycle discharge and charge capacities of MoS₂/G/Ag were 1605 and 1064 mAh g⁻¹, respectively (66% coulombic efficiency). The corresponding values for MoS₂/G were 1156 and 833 mAh g⁻¹ (72% coulombic efficiency). The higher first cycle capacity loss in MoS₂/G/Ag than in MoS₂/G led us to suspect that the Ag NCs might have catalyzed electrolyte

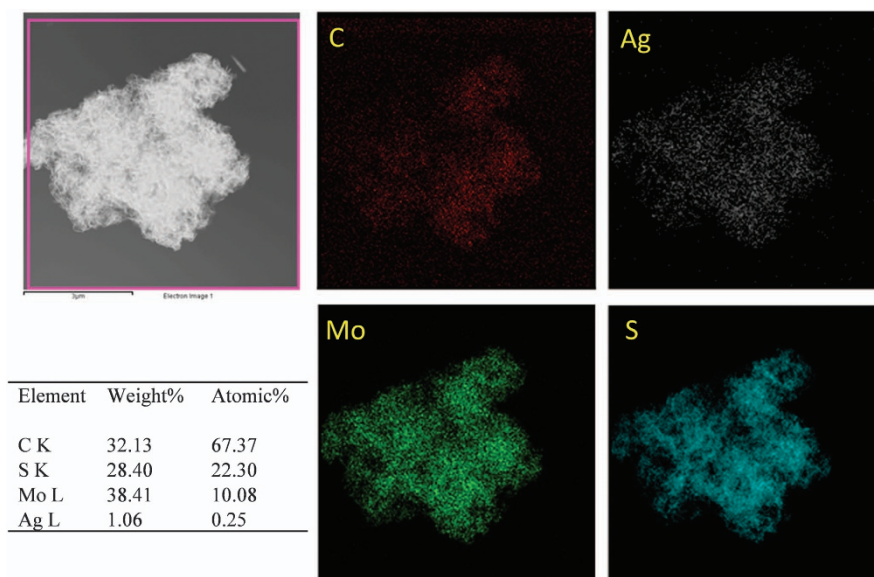


Figure 3 Elemental mapping and composition of MoS₂/G/Ag.

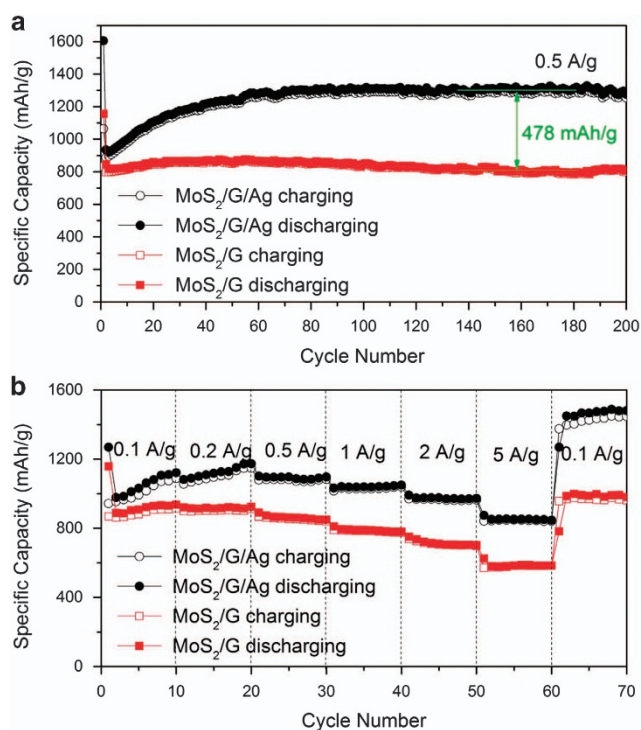


Figure 4 (a) Cycling performance of MoS₂/G and MoS₂/G/Ag (50 mA g⁻¹ for the first cycle and 500 mA g⁻¹ for the subsequent cycles), (b) rate performance of MoS₂/G and MoS₂/G/Ag.

decomposition. For confirmation, we analyzed the capacities in different voltage windows. Supplementary Figure S6 shows the voltage profiles of MoS₂/G/Ag and MoS₂/G electrodes in the 1st, 2nd, 5th, 50th and 100th cycles (again, at 50 mA g⁻¹ for the first cycle and 500 mA g⁻¹ thereafter). Three voltage plateaus appeared in the first discharge. The voltage plateau in the 1.2–0.75 V range should correspond to electrolyte reduction and Li⁺ intercalation into MoS₂ to form Li_xMoS₂.^{10,21} The voltage plateau in the 0.75–0.25 V region is

commonly attributed to the reduction of Li_xMoS₂ to Mo metal and Li₂S via a conversion reaction.^{10,21} The lowest voltage plateau in the 0.25–0.01 V region matches well with the insertion of Li⁺ into the graphene layers.^{10,21} The specific capacities in the 1.2–0.75, 0.75–0.25 and 0.25–0.01 V voltage windows were 160, 254 and 460 mAh g⁻¹, respectively, for MoS₂/G in the first discharge cycle and were 380, 683 and 300 mAh g⁻¹, respectively, for MoS₂/G/Ag. The comparison shows that the capacity in the 1.2–0.75 V region was higher for MoS₂/G/Ag. Because there is no feasible reason why the capacity due to intercalation should differ between composites that contain the same Li storage host, the higher value for MoS₂/G/Ag was most likely caused by a greater extent of electrolyte decomposition on this composite. The measurements also showed that the capacity corresponding to MoS₂ decomposition (0.75–0.25 V) was much higher in MoS₂/G/Ag than in MoS₂/G, which we rationalize as the catalyzed decomposition of MoS₂ by the Ag NCs. Metal-catalyzed electrochemical decomposition of a solid oxide is not common but has been observed in the decomposition of GeO₂ to Ge metal.³⁵

In subsequent cycles, the discharge capacity of MoS₂/G/Ag increased from 935 mAh g⁻¹ in the 2nd cycle to ~1300 mAh g⁻¹ in the 70th cycle and was stable thereafter. The discharge capacity of MoS₂/G was fairly constant at ~850 mAh g⁻¹ for the first 100 cycles and decreased to ~800 mAh g⁻¹ by the 200th cycle. The average capacity difference between MoS₂/G/Ag and MoS₂/G was 478 mAh g⁻¹ after 70 cycles. Thus, the addition of only 1 wt% of Ag NCs to MoS₂/graphene composite was able to increase the Li⁺ storage capacity by 60%. The coulombic efficiency was the same for MoS₂/G/Ag and MoS₂/G in every cycle. Hence, the dissimilarity was due to the difference in discharge capacity (lithiation capacity) in each cycle. The analysis of the voltage plateaus in different potential regions was again used to gain some insights into the function of Ag NCs in capacity enhancement.

In contrast to the 1st cycle, there were four voltage plateaus in the discharge curve from the 2nd to the 200th cycles. The voltage plateau in the 2.5–1.5 V region should correspond to the formation of Li₂S. The voltage plateaus in the 1.5–0.75 V and 0.75–0.25 V regions have been attributed to the association of Li⁺ with Mo.^{10,14} We thus expected that the association of Li⁺ with Ag NCs would also occur in

the same region. The voltage plateau in the 0.25–0.01 V region was the same as before and hence could be assigned to the storage of Li⁺ in graphene.^{10,14} From the comparison of the specific discharge capacities in the four voltage regions for the 2nd and 50th cycles (Supplementary Table S1), the effect of cycling on specific discharge capacity was not large for MoS₂/G. On the contrary, the specific capacities corresponding to Li₂S formation, the association of Li with Mo/Ag and the insertion of Li⁺ into graphene layers had all increased significantly with cycling in the presence of the Ag NCs. Taking the discharge capacity in the 100th cycle as an example, the overall specific capacities were 849 mAh g⁻¹ for MoS₂/G and 1308 mAh g⁻¹ for MoS₂/G/Ag. Hence, the addition of a minute quantity of Ag NCs (1 wt%) increased the overall Li⁺ storage capacity by 54%. Accordingly, the specific capacity corresponding to Li₂S formation increased from 232 mAh g⁻¹ for MoS₂/G to 248 mAh g⁻¹ for MoS₂/G/Ag, which constitutes a 2% increase compared with the original MoS₂/G. The specific capacity corresponding to the association of Li⁺ with Mo was 416 mAh g⁻¹ for MoS₂/G and increased to 671 mAh g⁻¹ for MoS₂/G/Ag due to the added possibility of associating with Ag. The increase of the MoS₂/G capacity was a rather substantial 30%. Finally, the specific capacity for Li⁺ insertion into graphene also increased from 201 mAh g⁻¹ for MoS₂/G to 390 mAh g⁻¹ for MoS₂/G/Ag, which constitutes a 22% increase over the original MoS₂/G capacity. The increase in capacity due to Li₂S formation could be posited as Ag NC-assisted immobilization of S. The increase in capacity in the Li-Mo association region could be due to the association of Li⁺ with Ag NCs, which have a large surface area for surface adsorption. The increase in capacity corresponding to the insertion of Li⁺ in graphene could be

attributed to the pillaring effect of Ag NCs in expanding the interlayer distance of graphene. Previous studies have shown that the Li storage capacity of graphene could be increased by expanding the interlayer distance.³⁶ A schematic showing the various functions of Ag NCs in MoS₂/G/Ag is given in Figure 1.

The MoS₂/G/Ag composite also exhibited improved rate performance. For example, the discharge capacities were still as high as 1040 and 850 mAh g⁻¹ when the current densities were increased to 1 and 5 A g⁻¹, respectively. At these higher current densities, the capacities of MoS₂/G were only 790 and 580 mAh g⁻¹ (Figure 4b). The rate performance of MoS₂/G/Ag is much better than most reported MoS₂-based composites, according to our literature survey, as shown in Supplementary Table S2. This may be due to the increased separation of the graphene sheets in the presence of Ag NCs. Because the mole ratio of Mo to C was approximately 1:6, the graphene sheets were few-layer in structure, and the interlayer distance should have thus been the same as that of graphite in MoS₂/G. The presence of intervening Ag NCs between adjacent graphene layers in MoS₂/G/Ag, however, could expand the interlayer distance to result in more facile Li⁺ transport. When the current density was returned to 0.1 A g⁻¹, a discharge capacity as high as ~1400 mAh g⁻¹ could still be obtained. This value is higher than any previously reported for MoS₂ composites. All of the previously stated reasons (the immobilization of S by Ag, the association of Li⁺ with Ag and the increase in the distance between the graphene sheets) have contributed to the collective increase in storage capacity beyond what is possible with only the conversion reaction $S + 2Li^+ \rightleftharpoons Li_2S$.

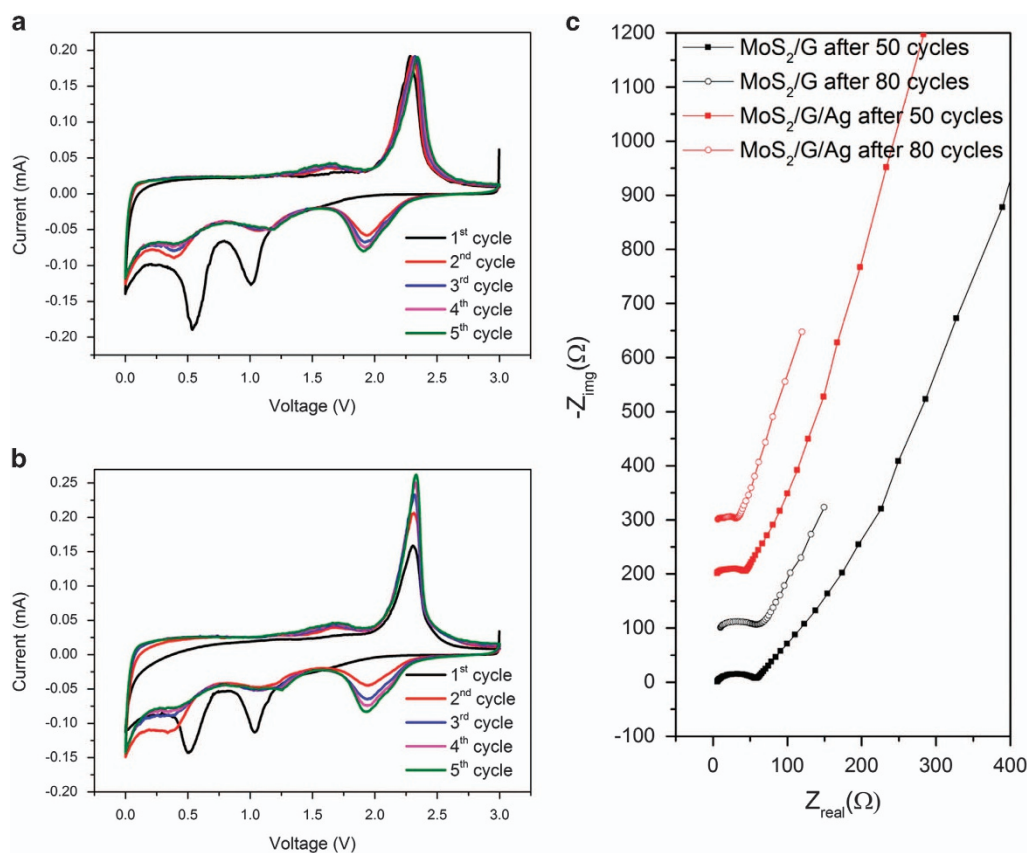


Figure 5 Cyclic voltammograms of MoS₂/G (a) and MoS₂/G/Ag (b) at 0.1 mV s⁻¹ for the first five cycles, (c) Nyquist plots of MoS₂/G and MoS₂/G/Ag electrodes after 50 and 80 cycles.

The electrochemical properties of the two composites were further analyzed by cyclic voltammetry measurements in the 0–3 V potential region at a scan rate of 0.1 mV s⁻¹ (Figures 5a,b). All reduction peaks appeared within the discharge voltage plateau regions discussed in the last section. There was only one strong oxidation peak at 2.3 V in the first delithiation cycle, corresponding well with the oxidation of Li₂S to S. One more peak, which appeared from the 2nd cycle onwards, may be associated with the disassociation of Li from Mo/Ag.¹⁰ A comparison of the voltammetric features shows an increase in the peak intensities of the reduction peak at 1.9 V and of the oxidation peak at 2.3 V with cycling for MoS₂/G/Ag but shows no changes for MoS₂/G. This corroborates the earlier observation of an increase in the capacity of the Li–S reactions with cycling in the presence of Ag NCs. The MoS₂/G and MoS₂/G/Ag composites after being discharged and charged for 50 and 80 cycles were also analyzed by electrochemical impedance spectroscopy. The Nyquist plots (Figure 5c) of the MoS₂/G/Ag electrode show generally smaller high to middle frequency semicircles characteristic of the overall charge transfer resistance in the electrode reaction. Because the electrical conductivity of Ag NCs is not high,³⁷ the observed capacity increase was likely due to the contributions of Ag NCs in Li⁺ conduction and storage rather than electron conduction. The Nyquist plots show a decrease in charge transfer resistance with cycling for MoS₂/G/Ag and a nearly invariant charge transfer resistance for MoS₂/G. This mirrors the trend of increasing specific capacity of MoS₂/G/Ag with cycling in the first 70 cycles. Earlier, we mentioned that the higher capacity of MoS₂/G/Ag was due to the roles of Ag NCs in S immobilization, their association with Li⁺ ions and the increase in the interlayer distance between the graphene sheets. The gradual capacity increase in the first 70 cycles has the appearance of an activation process, the origin of which is unknown. We suppose that the strong affinity between Ag and S may play a role in this process.

CONCLUSIONS

A ternary composite of graphene, MoS₂ nanosheets and silver NCs (MoS₂/G/Ag), was prepared by depositing Ag NCs on GO sheets before the formation of MoS₂ layers. Because the internalization of Ag NCs in this system consists only of mixing GO and the silver precursor in an aqueous solution followed by CO reduction, this additional synthetic step is relatively simple and can be easily scaled up. A small amount of Ag NCs (1 wt% Ag in MoS₂/G/Ag) uniformly dispersed in the composite was found to significantly improve the electrochemical properties of MoS₂/G as a Li⁺ storage host. When cycled at a current density of 0.5 A g⁻¹, the discharge capacity of MoS₂/G/Ag increased from 935 mAh g⁻¹ in the 2nd cycle to ~1300 mAh g⁻¹ in the 70th cycle and was stable thereafter. By comparison, the discharge capacity of MoS₂/G without the Ag NCs was fairly constant at ~800–850 mAh g⁻¹ in the same number of cycles. Hence, the average increase in the capacity of MoS₂/G after Ag NC modification was a noticeable 478 mAh g⁻¹ at the steady state. The improved electrochemical performance of MoS₂/G/Ag could be attributed to a number of effects brought about by the Ag NCs: the immobilization of S, the association of Li⁺ and the increase in the distance between the graphene sheets. In addition to higher capacity, MoS₂/G/Ag exhibited enhanced rate performance: discharge capacities as high as 1040 and 850 mAh g⁻¹, even at the elevated current densities of 1 and 5 A g⁻¹, respectively. These capacities compare very favourably with the corresponding values from MoS₂/G, which were only 790 and 580 mAh g⁻¹.

CONFLICT OF INTEREST

The authors declare no conflict of interest.

ACKNOWLEDGEMENTS

This work was financially supported by the A*STAR Project 1220203049 (R279-000-370-305), the International Science and Technology Cooperation Program of China (2012DFG42100), the Natural Science Foundation of China (21173190, 21473156), the Doctoral Program of Higher Education of China (2011010113003) and the International Science and Technology Cooperation Program of Zhejiang Province (2013C24011).

- Ramakrishna Matte, H. S. S., Gomathi, A., Manna, A. K., Late, D. J., Datta, R., Pati, S. K. & Rao, C. N. MoS₂ and WS₂ analogues of graphene. *Angew. Chem. Int. Ed.* **49**, 4059–4062 (2010).
- Chhowalla, M., Shin, H. S., Eda, G., Li, L.-J., Loh, K. P. & Zhang, H. The chemistry of two-dimensional layered transition metal dichalcogenide nanosheets. *Nat. Chem.* **5**, 263–275 (2013).
- Kim, S., Konar, A., Hwang, W.-S., Lee, J. H., Lee, J., Yang, J., Jung, C., Kim, H., Yoo, J. B., Choi, J. Y., Jin, Y. W., Lee, S. Y., Jena, D., Choi, W. & Kim, K. High-mobility and low-power thin-film transistors based on multilayer MoS₂ crystals. *Nat. Commun.* **3**, 1011 (2012).
- Kibsgaard, J., Chen, Z., Reinecke, B. N. & Jaramillo, T. F. Engineering the surface structure of MoS₂ to preferentially expose active edge sites for electrocatalysis. *Nat. Mater.* **11**, 963–969 (2012).
- Fuhrer, M. S. & Hone, J. Measurement of mobility in dual-gated MoS₂ transistors. *Nat. Nanotechnol.* **8**, 146–147 (2013).
- Lauritsen, J. V., Kibsgaard, J., Helveg, S., Topsoe, H., Clausen, B. S., Laegsgaard, E. & Besenbacher, F. Size-dependent structure of MoS₂ nanocrystals. *Nat. Nanotechnol.* **2**, 53–58 (2007).
- Geim, A. K. & Grigorieva, I. V. Van der Waals heterostructures. *Nature* **499**, 419–425 (2013).
- Xiao, J., Choi, D., Cosimbescu, L., Koech, P., Liu, J. & Lemmon, J. P. Exfoliated MoS₂ nanocomposite as an anode material for lithium ion batteries. *Chem. Mater.* **22**, 4522–4524 (2010).
- Hwang, H., Kim, H. & Cho, J. MoS₂ nanoplates consisting of disordered graphene-like layers for high rate lithium battery anode materials. *Nano Lett.* **11**, 4826–4830 (2011).
- Xiao, J., Wang, X., Yang, X.-Q., Xun, S., Liu, G., Koech, P. K., Liu, J. & Lemmon, J. P. Electrochemically induced high capacity displacement reaction of PEO/MoS₂/graphene nanocomposites with lithium. *Adv. Funct. Mater.* **21**, 2840–2846 (2011).
- Chang, K. & Chen, W. L-cysteine-assisted synthesis of layered MoS₂/graphene composites with excellent electrochemical performances for lithium ion batteries. *ACS Nano* **5**, 4720–4728 (2011).
- Chang, Y.-H., Lin, C.-T., Chen, T.-Y., Hsu, C.-L., Lee, Y.-H., Zhang, W., Wei, K. H. & Li, L. J. Highly efficient electrocatalytic hydrogen production by MoS₂ grown on graphene-protected 3D Ni foams. *Adv. Mater.* **25**, 756–760 (2013).
- Zhu, C., Mu, X., van Aken, P. A., Yu, Y. & Maier, J. Single-layered ultrasmall nanoplates of MoS₂ embedded in carbon nanofibers with excellent electrochemical performance for lithium and sodium storage. *Angew. Chem. Int. Ed.* **53**, 2152–2156 (2014).
- Gong, Y., Yang, S., Zhan, L., Ma, L., Vajtai, R. & Ajayan, P. M. A bottom-up approach to build 3D architectures from nanosheets for superior lithium storage. *Adv. Funct. Mater.* **24**, 125–130 (2014).
- Lian, P., Zhu, X., Liang, S., Li, Z., Yang, W. & Wang, H. Large reversible capacity of high quality graphene sheets as an anode material for lithium-ion batteries. *Electrochim. Acta* **55**, 3909–3914 (2010).
- Wu, Z.-S., Ren, W., Xu, L., Li, F. & Cheng, H.-M. Doped graphene sheets as anode materials with superhigh rate and large capacity for lithium ion batteries. *ACS Nano* **5**, 5463–5471 (2011).
- Chang, K. & Chen, W. In situ synthesis of MoS₂/graphene nanosheet composites with extraordinarily high electrochemical performance for lithium ion batteries. *Chem. Commun.* **47**, 4252–4254 (2011).
- Chang, K. & Chen, W. Single-layer MoS₂/graphene dispersed in amorphous carbon: Towards high electrochemical performances in rechargeable lithium ion batteries. *J. Mater. Chem.* **21**, 17175–17184 (2011).
- Chang, K., Chen, W., Ma, L., Li, H., Li, H., Huang, F., Xu, Z., Zhang, Q. & Lee, J. Y. Graphene-like MoS₂/amorphous carbon composites with high capacity and excellent stability as anode materials for lithium ion batteries. *J. Mater. Chem.* **21**, 6251–6257 (2011).
- Chang, K., Geng, D., Li, X., Yang, J., Tang, Y., Cai, M., Li, R. & Sun, X. Ultrathin MoS₂/nitrogen-doped graphene nanosheets with highly reversible lithium storage. *Adv. Energy Mater.* **3**, 839–844 (2013).
- Stephenson, T., Li, Z., Olsen, B. & Mitlin, D. Lithium ion battery applications of molybdenum disulfide (MoS₂) nanocomposites. *Energy Environ. Sci.* **7**, 209–231 (2014).

- 22 Bakr, O. M., Amendola, V., Aikens, C. M., Wenseleers, W., Li, R., Dal Negro, L., Schatz, G. C. & Stellacci, F. Silver nanoparticles with broad multiband linear optical absorption. *Angew. Chem. Int. Ed.* **48**, 5921–5926 (2009).
- 23 Choi, S., Dickson, R. M. & Yu, J. Developing luminescent silver nanodots for biological applications. *Chem. Soc. Rev.* **41**, 1867–1891 (2012).
- 24 Desireddy, A., Conn, B. E., Guo, J., Yoon, B., Barnett, R. N., Monahan, B. M., Kirschbaum, K., Griffith, W. P., Whetten, R. L., Landman, U. & Bigioni, T. P., Ultrastable silver nanoparticles. *Nature* **501**, 399–402 (2013).
- 25 Yang, H., Wang, Y., Huang, H., Gell, L., Lehtovaara, L., Malola, S., Häkkinen, H. & Zheng, N. All-thiol-stabilized Ag₄₄ and Au₁₂Ag₃₂ nanoparticles with single-crystal structures. *Nat. Commun.* **4**, 2422 (2013).
- 26 Yuan, X., Setyawati, M. I., Tan, A. S., Ong, C. N., Leong, D. T. & Xie, J. Highly luminescent silver nanoclusters with tunable emissions: cyclic reduction-decomposition synthesis and antimicrobial properties. *NPG Asia Mater.* **5**, e39 (2013).
- 27 Chakraborty, I., Kurashige, W., Kanehira, K., Gell, L., Häkkinen, H. J., Negishi, Y. & Pradeep, T. Ag₄₄(SeR)₃₀: A hollow cage silver cluster with selenolate protection. *J. Phys. Chem. Lett.* **4**, 3351–3355 (2013).
- 28 Chen, D., Ji, G., Ding, B., Ma, Y., Qu, B., Chen, W. & Lee, J. Y. *In situ* nitrogenated graphene-few-layer WS₂ composites for fast and reversible Li⁺ storage. *Nanoscale* **5**, 7890–7896 (2013).
- 29 Yu, Y., Luo, Z., Yu, Y., Lee, J. Y. & Xie, J. Observation of cluster size growth in co-directed synthesis of Au₂₅(SR)₁₈ nanoclusters. *ACS Nano* **6**, 7920–7927 (2012).
- 30 Zhou, X., Wang, Z., Chen, W., Ma, L., Chen, D. & Lee, J. Y. Facile synthesis and electrochemical properties of two dimensional layered MoS₂/graphene composite for reversible lithium storage. *J. Power Sources* **251**, 264–268 (2014).
- 31 Zhang, Z., Xu, F., Yang, W., Guo, M., Wang, X., Zhang, B. & Tang, J. A facile one-pot method to high-quality Ag-graphene composite nanosheets for efficient surface-enhanced raman scattering. *Chem. Commun.* **47**, 6440–6442 (2011).
- 32 Zhang, Y., Liu, S., Wang, L., Qin, X., Tian, J., Lu, W., Chang, G. & Sun, X. One-pot green synthesis of Ag nanoparticles-graphene nanocomposites and their applications in SERS, H₂O₂, and glucose sensing. *RSC Adv.* **2**, 538–545 (2012).
- 33 Yu, Y., Chen, X., Yao, Q., Yu, Y., Yan, N. & Xie, J. Scalable and precise synthesis of thiolated Au_{10–12}, Au₁₅, Au₁₈, and Au₂₅ nanoclusters via pH controlled CO reduction. *Chem. Mater.* **25**, 946–952 (2013).
- 34 Huang, G., Chen, T., Chen, W., Wang, Z., Chang, K., Ma, L., Huang, F., Chen, D. & Lee, J. Y. Graphene-like MoS₂/graphene composites: Cationic surfactant-assisted hydrothermal synthesis and electrochemical reversible storage of lithium. *Small* **9**, 3693–3703 (2013).
- 35 Seng, K. H., Park, M.-h., Guo, Z. P., Liu, H. K. & Cho, J. Catalytic role of Ge in highly reversible GeO₂/Ge/C nanocomposite anode material for lithium batteries. *Nano Lett.* **13**, 1230–1236 (2013).
- 36 Yoo, E., Kim, J., Hosono, E., Zhou, H.-S., Kudo, T. & Honma, I. Large reversible Li storage of graphene nanosheet families for use in rechargeable lithium ion batteries. *Nano Lett.* **8**, 2277–2282 (2008).
- 37 Chen, S., Ingram, R. S., Hostetler, M. J., Pietron, J. J., Murray, R. W., Schaaff, T. G., Khoury, J. T., Alvarez, M. M. & Whetten, R. L. Gold nanoelectrodes of varied size: Transition to molecule-like charging. *Science* **280**, 2098–2101 (1998).



This work is licensed under a Creative Commons Attribution 4.0 International License. The images or other third party material in this article are included in the article's Creative Commons license, unless indicated otherwise in the credit line; if the material is not included under the Creative Commons license, users will need to obtain permission from the license holder to reproduce the material. To view a copy of this license, visit <http://creativecommons.org/licenses/by/4.0/>

Supplementary Information accompanies the paper on the NPG Asia Materials website (<http://www.nature.com/am>)